Math. Model. Nat. Phenom. 13 (2018) 51
https://doi.org/10.1051/mmnp/2018046

Mathematical Modelling of Natural Phenomena
www.mmnp-journal.org

MECHANISMS PERFORMANCE AND PRESSURE DEPENDENCE OF HYDROGEN/AIR BURNER-STABILIZED FLAMES[☆]

V. Bykov[1,*], V.V. Gubernov[2] and U. Maas[1]

Abstract. The kinetic mechanism of hydrogen combustion is the most investigated combustion system. This is due to extreme importance of the mechanism for combustion processes, *i.e.* it is present as a sub-mechanism in all mechanisms for hydrocarbon combustion systems. Therefore, detailed aspects of hydrogen flames are still under active investigations, *e.g.* under elevated pressure, under conditions of different heat losses intensities and local equivalence ratios etc. For this purpose, the burner stabilized flame configuration is an efficient tool to study different aspects of chemical kinetics by varying the stand-off distance, pressure, temperature of the burner and mixture compositions.

In the present work, a flat porous plug burner flame configuration is revisited. A hydrogen/air combustion system is considered with detailed molecular transport including thermo-diffusion and with 8 different chemical reaction mechanisms. Detailed numerical investigations are performed to single out the role of chemical kinetics on the loss of stability and on the dynamics of the flame oscillations. As a main outcome, it was found/demonstrated that the results of critical values, *e.g.* critical mass flow rate, weighted frequency of oscillations and blow-off velocity, with increasing the pressure scatter almost randomly. Thus, these parameters can be considered as independent and can be used to improve and to validate the mechanisms of chemical kinetics for the unsteady dynamics.

Mathematics Subject Classification. 80A25, 80A30

Received April 15, 2018. Accepted June 21, 2018.

1. Introduction

There is an increasing demand for reliable combustion mechanisms describing transient regimes of combustion near the stability limits. In view of recent progress made in the detailed modeling (*e.g.* molecular transport, chemical kinetics etc.) and in numerical integration a very detailed solution even for unsteady combustion regimes has become available. In this respect, the behavior of burner-stabilized flames, which is one of most investigated configurations of combustion theory, remains open. Burner stabilized flames provide a unique opportunity to directly compare the results of numerical modeling and experiments (see *e.g.* [11, 18] for relevant detailed review of the experimental studies) even for transient regimes of combustion. Due to the very simple

[☆] The authors acknowledge the support from DFG-RFBR grant number 17-53-12018 (RFBR)/ BY 94/2 – 1 (DFG). VVG acknowledges the support of RFBR grant numbers 17-01-00070, 16-03-00758.

Keywords and phrases: Chemical kinetics, premixed laminar flames, burner-stabilized flames, pulsating instability, hydrogen-air combustion

[1] Karlsruhe Institute of Technology (KIT), Institute of Technical Thermodynamics, Engelbert-Arnold-Strasse 4, Building 10.91, D-76131 Karlsruhe, Germany.
[2] P.N. Lebedev Physical Institute of Russian Academy of Sciences, Moscow 119991, 53 Leninskii prosp., Russian Federation.

[*] Corresponding author: viatchelsav.bykov@kit.edu

geometry and the possibility to access the flame structure by using different direct and indirect measurements (the flame height, speed, structure of the flame) the flame dynamics can be investigated experimentally. Moreover, the flame can be efficiently controlled and maintained at different regimes. This can be used to verify the reaction as well as transport models similarly as in [21] and to study various combustion regimes [1, 12, 15].

As to our knowledge, the mechanisms of combustion of hydrogen in this configuration are verified under low, atmospheric and moderately elevated (up to 5 atm) pressures [21]. Nevertheless, understanding the chemistry of hydrogen oxidation at high pressure and near the stability limits conditions is crucial for applications in development of engines and propulsion [4]. Therefore, the development of reliable mechanisms of chemical kinetic describing such combustion system represents a very interesting and challenging task.

The properties, stability and pulsating dynamics of one-dimensional flame fronts stabilized over a flat burner are very well investigated qualitatively in a number of analytic papers using asymptotic analysis (see *e.g.* [3, 8, 19, 29]).

The flame stability analysis by using the activation energy asymptotic approach is provided *e.g.* in [27]. It was shown that the flame-wall interaction between the hot reacting gas and burner can significantly promote the onset of pulsating instabilities, while in [29] the emergence of one-dimensional pulsating instabilities is reported and studied under assumption of an infinitely thin burner, which played a role of a heat sink. In [3], the asymptotic analysis was carried out in the nearly equally-diffusional approximation, however, different models of the burner have been used. Mixed boundary conditions were imposed for the mass fraction of fuel taking into account the depletion of fuel concentration inside of the burner due to diffusion. Several conclusions on the characteristics of pulsating instabilities can be drawn based on the results obtained in [3]. Namely, the heat exchange with the burner significantly promotes the onset of flame pulsations: it is possible to encounter flame oscillations for mixtures with Lewis number less than one, the stationary planar flame may become completely unstable for all values of the Lewis number, the dominating type of oscillatory instability is planar one-dimensional. The latter is of principal importance for our investigations. The dynamics of flame oscillations for mixtures with Lewis number equal to one was studied in [19], where an evolution equation for the location of the flame front was derived. It was shown that the low-temperature branch is unstable, while the high-temperature branch looses stability before the minimum stand-off distance is reached and flame pulsations emerge as a result of the supercritical Hopf bifurcation. All these conclusions qualitatively agree with the results of detailed numerical simulations of burner stabilized hydrogen-oxygen flame calculated with the thirteen step skeletal mechanism for rich mixture under ambient pressure and elevated temperature of the burner [27].

In [22], the stability of the burner stabilized flame is revisited to take into consideration the transport processes inside of the porous media of the burner. The investigation is carried out both analytically and numerically using flame-sheet and finite rate chemistry assumptions, respectively. It was demonstrated that the burner thickness and porosity can affect the flame stability. In particular, if the ratio of burner plate thickness in units of flame thickness to its porosity is finite, then the low-temperature branch of solutions can regain the stability for sufficiently large stand-off distances. The effect of radiation or volumetric linear heat losses on burner stabilized flame properties and stability was studied in *e.g.* [5, 23]. It was demonstrated that the region of existence of steady solutions in the space of parameters shrinks with the intensification of heat losses, which eventually leads to flame quenching. Moreover, the heat losses also promote the onset of both pulsating and cellular instabilities.

Note, however, that most of the studies of unsteady burner-stabilized flames have been performed within the framework of single-step reaction, *e.g.* [27, 28]. Therefore, in our earlier paper [17] a detailed study of the unsteady process has been performed for several detailed kinetic mechanisms and transport models. The detailed study of the influence of the main system parameters on the onset and on the dynamics of oscillating regime are provided in this work. Several important conclusion are drawn which motivate current investigations, namely, theoretical predictions of two branches (U-shaped solution), the high-temperature (or fast) and low-temperature (or slow) branches are confirmed, such that between them the condition of the minimum stand-off distance is realized. As the mass flow rate tends to the value corresponding to the freely propagating adiabatic flame speed, the stand-off distance grows and the blow-off occurs. At the slow solution branch the flame height also exhibits "blow-off" – extinguished as the mass flow rate vanishes. Additionally, it is found that the U-shaped solution can be completely stable, fully unstable or partly stable with respect to oscillatory instabilities depending mainly on

the equivalence ratio. It is also demonstrated in [17] that the lower and upper bounds for the range of existence of the stationary flame front in terms of the critical values of the mass flow rate strongly depend on system parameters. Moreover, the choice of reaction mechanisms strongly affects the prediction of the values of the critical parameters for the onset of pulsating instabilities and blow-off as well as frequency of flame oscillations and the disparity between the results for different mechanisms increases as the pressure is increased.

The purpose of the current study is to extend these results by using recently developed mechanisms developed to address higher pressures as well as to explore possibilities to use outlined regimes as a source for additional validation and improvement of detailed mechanisms. A number of key parameters, which can be easily controlled in experiments by varying mixture composition, temperature of the burner, pressure etc., are figured out. In order to verify this, special attention is paid to predictions obtained with different kinetic mechanisms to ensure the independent character of the specified parameters that can be measured additionally in the experiment to validate mechanisms of chemical kinetic of combustion in general and of hydrogen air combustion system in particular.

2. Mathematical model, mechanisms and numerical method

The mathematical model for burner stabilized one-dimensional flame can be found elsewhere *e.g.* in [16, 27]. In the current work, it is implemented for modeling and numerical study of a flat burner and includes detailed chemical mechanisms and detailed transport models. The system is described by spatially one-dimensional conservation equations of mass, energy and species conservation as well as the ideal gas state equation. Formally the system of governing equations can be written as

$$\begin{aligned}
&\frac{\partial \rho}{\partial t} + \frac{\partial \dot{m}}{\partial x} = 0, \\
&\rho c_p \frac{\partial T}{\partial t} + c_p \dot{m} \frac{\partial T}{\partial x} = \frac{\partial}{\partial x}\left(\lambda \frac{\partial T}{\partial x}\right) - \sum_j h_j r_j, \\
&\rho \frac{\partial Y_i}{\partial t} + \dot{m} \frac{\partial Y_i}{\partial x} + \frac{\partial j_i}{\partial x} = r_i,
\end{aligned} \tag{2.1}$$

where t and x is the time and spacial coordinate, T is the temperature, Y_i is the mass fraction of species i, ρ, c_p, and λ are the density, the specific heat, and the heat conductivity of the mixture, respectively; $\dot{m} = \rho v$ is the mass flow rate – (mass flux density), r_i, h_i, and j_i is the chemical rate of production, the specific enthalpy, and the diffusion flux of species i.

In order to close the system and specify boundary conditions the following configuration of the combustion system is considered. The outlet surface of the flat burner is located at $x = 0$. To the left from it ($x < 0$) the space is filled with the porous medium through, which the fresh mixture is supplied. Robin boundary conditions are applied for the species at the outlet gas-solid interface [27]. These mixed boundary conditions account for the flux of the mass fraction of species at the burner entrance and diffusive flux at $x = 0$. The temperature of the fresh mixture at $x = 0$ is assumed to be equal to the burner temperature T_0

$$\begin{aligned}
&T = T_0, \quad \dot{m} Y_i + j_i = \dot{m} Y_i^0, && \text{for } x = 0, \\
&\frac{\partial T}{\partial x} = 0, \quad \frac{\partial Y_i}{\partial x} = 0, && \text{for } x = \infty,
\end{aligned} \tag{2.2}$$

where Y_i^0 denotes the mass fraction of species i in the fresh mixture, which is fed into the burner.

Several basic assumptions have been made typical for laminar flames, namely, the uniform pressure assumption was used, and because the burner is considered to have a large thermal inertia and thickness, which is much larger than the thermal thickness of the flame, the porous plate is assumed to be at constant temperature. The later can be achieved in experiments *e.g.* by using a water cooling system [2, 30]. Additionally, it has to be mentioned here that the heterogeneous reactions are neglected as well, although they can be easily included

into the consideration and implemented already in the program. In several parametric studies we noticed that at such low temperatures there is no influence of surface catalytic reactions on the structure as well as on the dynamics of the considered flames.

In the current study, we consider the case of flat one-dimensional combustion fronts only. It is known that the dynamics of flames stabilized on porous plug burners can lead to the formation of two-dimensional spacial structures [1, 2, 12, 15]. Nevertheless, the stability analysis of burner stabilized flames in [3, 22] clearly shows that in the case of Lewis number greater than one the dominating type of instability is planar pulsating one-dimensional. Thus using the one-dimensional model is justified for the case of rich hydrogen-air flames, which are characterised by the overall Lewis number greater than one. The radiation heat losses are neglected in the current consideration. As flame approaches the surface of the burner closely and pulsations are expected to occur, the heat loss is mostly governed by the flame-wall thermal interaction. Thus we expect that the characteristics of flame pulsations are not sensitive to the radiative heat losses in this case.

2.1. Mechanisms, transport model

A number (8) of detailed chemical reaction mechanisms is considered, namely, Warnatz [25, 34], San-Diego [31], GRI3.0 [32], Keromnes [20], Li [24], USC2.0 [36]. All these well-established mechanisms have been extensively validated. Moreover, two additional mechanisms are considered: one was specially developed for high pressure [4] and the other [35] is the result of a comparison of all known and widely used hydrogen combustion mechanisms with subsequent optimization based on the reliable set of the experimental data.

The detailed molecular transport including thermal diffusion is taken into account in equation (2.1) for calculation of the flux j_i (see *e.g.* [25]) given by

$$j_i = -D_i^M \rho \frac{Y_i}{X_i} \frac{\partial X_i}{\partial x} - \frac{D_i^T}{T} \frac{\partial T}{\partial x}, \tag{2.3}$$

where additionally X_i is the molar fraction of species i, D_i^M is the diffusion coefficient for species i, D_i^T is the thermal diffusion coefficient. These equations are supplemented with the ideal gas equation of state. In numerical computations of equation (2.3) the so-called mixture averaged transport model with mass correction procedure based on the Curtiss-Hirschfelder approximation is used [13, 14, 18].

2.2. Numerical method

In order to simplify the implementation the system of conservation equations are treated in primitive variables with the density, the velocity, the temperature and the species mass fractions, as dependent variables. Furthermore, a Lagrangian type coordinate transformation is applied in order to avoid problems in describing the convective terms (see *e.g.* [33]). The numerical integration scheme used in this work has been reported elsewhere and can be found *e.g.* in [25, 26]. Briefly, the numerical integration is performed by employing the method of lines. Spatial discretization on statically adapted grids leads to a large system of coupled ordinary differential and algebraic equations (DAE). This DAEs system is integrated by an implicit extrapolation method with internal order and step-size control and error-estimation [9, 10]. The implicit integration and the suggested numerical scheme of the time step control allow us to simulate combustion processes very accurately.

3. Results and discussion

3.1. Flame characteristics

In this section, we describe the results of numerical calculations outlined in Section 2 of flame properties and pulsating dynamics. The main aim of this subsection is to qualitatively introduce the critical phenomena related to the burner stabilized flames and their characteristics. For this reason here the results are presented for just one reaction mechanism [25, 34]. The comparison of the predictions of different mechanisms is carried out in the next subsections. All the data presented here correspond to rich mixtures with equivalence ratio

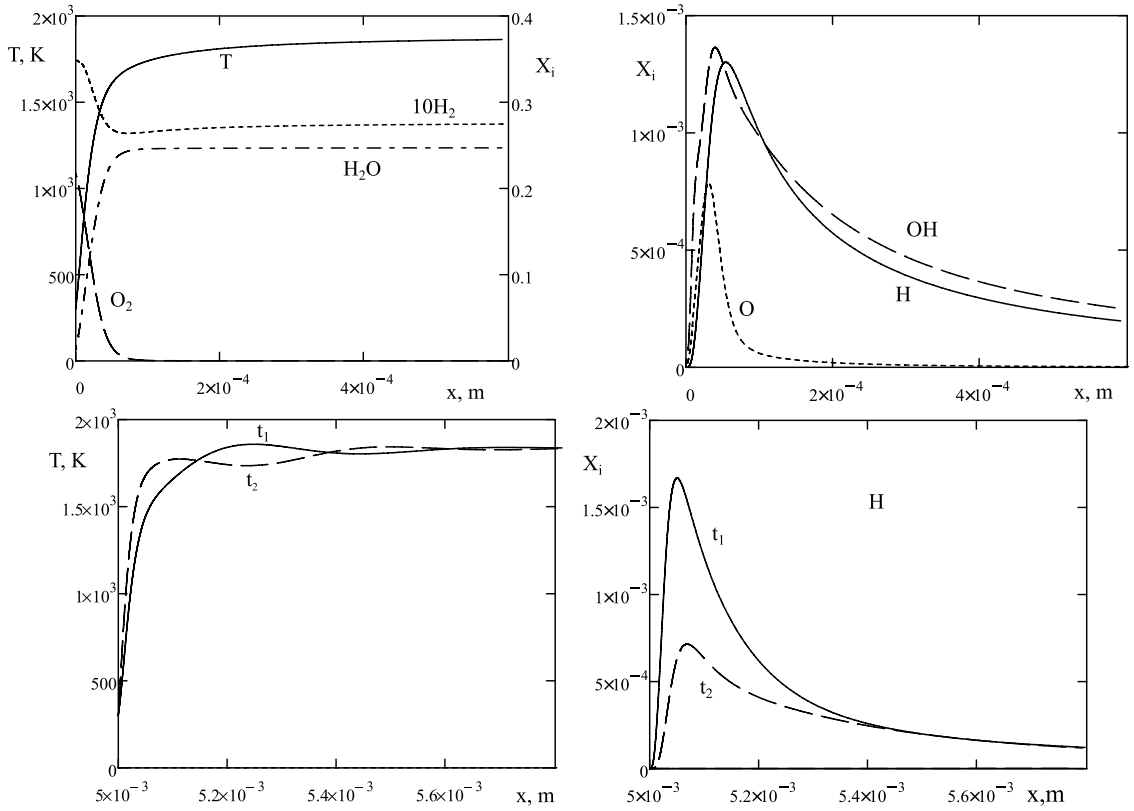

FIGURE 1. The structure of the burner stabilized flame for $\phi = 2$ and pressure $P = 5$ bar. The steady flame for $\dot{m} = 6$ kg/m^2 is illustrated in the top two figures, whereas the bottom figures show the flame pulsations for $\dot{m} = 5$ kg/m^2 at two moments of time $t_1 = 0$ and $t_2 = 0.022$ ms.

$\phi = 2$, since the oscillatory instability is preferentially observed in burner stabilized flames for rich mixtures. The temperature of the burner is fixed to the normal conditions, $T_0 = 298$ K, while ambient pressure and mass flow rate are varied.

The onset of flame oscillations is illustrated in Figure 1 for $\phi = 2$ and pressure $P = 5$ bar. The distribution of the temperature and molar fractions of reaction species is plotted in the top two figures for the case of steady solution at the mass flow rate $\dot{m} = 6$ kg/m^{2}s. In the top left figure the dependence of T, XH_2, O_2, H_2O on coordinate x is presented, while the distribution of the radical species molar fractions XH, O, OH is shown in the right top figure. If the mass flow rate is decreased down to $\dot{m} = 5$ kg/m^{2}s the flame oscillations occur. The temperature and molar fraction of H-radicals at two moments of time $t_1 = 0$ and $t_2 = 0.022$ ms are plotted in the bottom left and right figures, respectively. As seen $T(x,t)$ and $X_H(x,t)$ are non steady periodic functions of time. The oscillations of temperature 0.25 mm away from the surface of the burner is over 100 K while the maximum of H-radical distribution exhibits pulsations with much higher amplitude which is around 50% of the maximum value in the case of steady flame at $\dot{m} = 6$ kg/m^{2}s.

Flames stabilized on the flat burner are usually characterized by the distance of the flame position from the surface of the burner (or flame height), h. Here we define the flame position as the coordinate of the local peak in the molar fraction of H radicals. In Figure 2, the dependence of the flame height is plotted as function of the mass flow rate $\dot{m}$, for different values of pressure, $P = 2$, 5, and 10 bar. The steady flame location is shown with the solid lines. The critical values of $\dot{m}$ are plotted with the vertical dashed line and empty squares, whereas

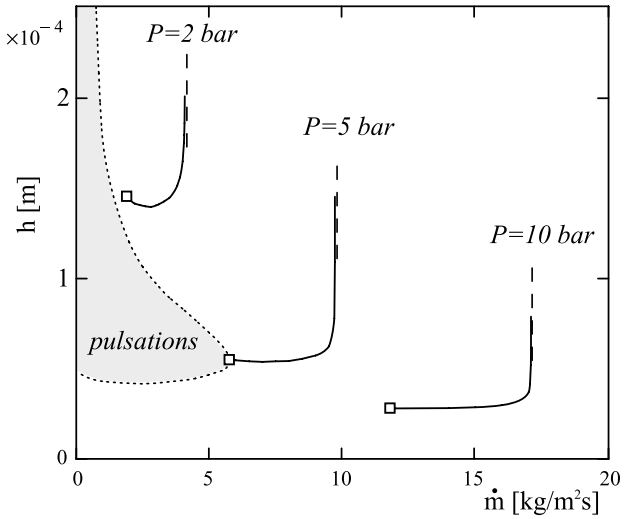

FIGURE 2. The dependence of flame height, h, on the mass flow rate, $\dot{m}$ for $\phi = 2$ and pressure $P = 2$, 5 and 10 bar. The vertical dashed lines represent the mass flow rates for the freely propagating combustion waves. Empty squares show the critical parameter values for the onset of oscillations. The shaded region bounded by the dotted line represents the range of variation of h in the pulsating solution for $P = 5$ bar.

the parameter values representing the pulsating solutions are illustrated for the case $P = 5$ bar as the shaded region bounded with the dotted line.

For each value of P as $\dot{m}$ is increased, the flame departs downstream and h grows until $\dot{m}$ approaches the value of the mass flow rate corresponding to the freely propagating deflagration wave and blow-off ($h \to \infty$) occurs. The latter is presented in Figure 2 with the vertical dashed lines. In the opposite limit, as $\dot{m}$ is decreased, the other critical phenomena occurs – the onset of flame pulsations. The characteristics of flame oscillations are illustrated in Figure 2 for $P = 5$ bar. The range of variation of h for pulsating solutions is demonstrated with the shaded area bounded by the dotted lines. The dotted lines indicate the minimal and maximal stand-off distance in oscillating flame for fixed $\dot{m}$. It is seen that as $\dot{m} < 1$ kg/m^{2}s or $\dot{m} \sim 1$ kg/m^{2}s the distance traveled by the pulsating flame becomes of the order of hundreds of microns. It is also important to note that the flame pulsations occur as the flame height decreases and the heat exchange between flame and burner is intensified. This is in contrast to the oscillations of freely propagating hydrogen-air deflagrations which emerge with the increase of the equivalence ratio even for the case of adiabatic flames [6, 7].

The parameter values corresponding to the loss of stability of steady flames are shown with the empty squares. It is seen that in cases $P = 2$ and 5 bar the function $h(\dot{m})$ passes through the minimal flame height before the onset of pulsations, whereas for $P = 10$ bar the curve $h(\dot{m})$ approaches the square symbol in a monotonic way *i.e.* before reaching the minimal stand-off condition. This implies that at normal and moderately elevated pressure, there exist two stable stationary solutions corresponding to the same flame height above that burner, however, characterized by different mass flow rates and flame burned temperatures. As the pressure is increased the solution branch with smaller $\dot{m}$ and flame burned temperature becomes completely unstable and only single stable steady solution exists (see *e.g.* [17]).

The dependence of the flame height above the burner on the mass flow rate is U-shaped function. The right branch of $h(\dot{m})$ function corresponding to the solutions departing from the burner surface as the mass flow rate is increased is completely stable for the values of pressure considered in this work. The left branch of the $h(\dot{m})$ function is unstable for the mass flow rate smaller than the values marked with the empty square, while there may occur a stable part of the left branch between the critical parameter values for the onset of pulsations and for the minimal stand-off distance (see Fig. 2 for $P = 2$ and 5 bar). In this case there may exist two stable

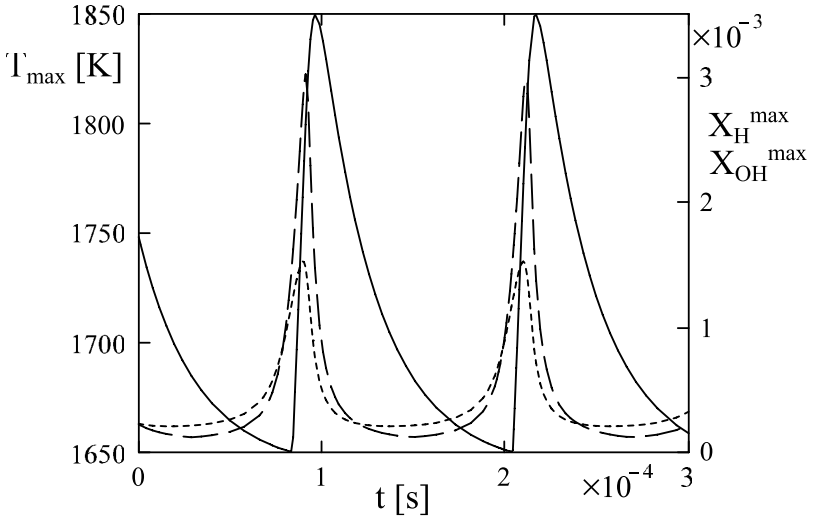

FIGURE 3. The amplitude of oscillations of local maxima of T (*solid line*), X_{H} (*dotted line*), and X_{OH} (*dashed line*) for $\phi = 2$, $\dot{m} = 2$ kg/m^{2}s, and $P = 5$ bar.

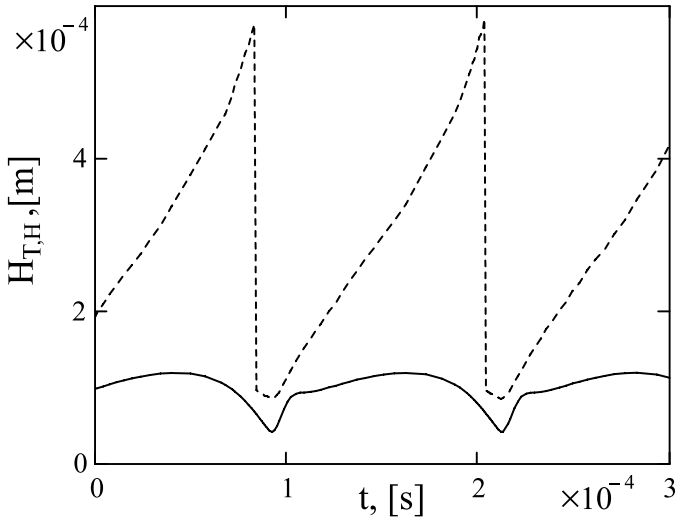

FIGURE 4. The distance $H_{T,H}$ of the local maximum of T (*dotted line*) and X_{H} (*solid line*) from the burner surface for $\phi = 2$, $\dot{m} = 2$ kg/m^{2}s, and $P = 5$ bar.

stationary solutions for the same flame height above that burner characterized by different mass flow rates $\dot{m}_1$ (left branch) and $\dot{m}_1$ (right branch) so that $h(\dot{m}_1) = h(\dot{m}_2)$. As pressure is increased up to a certain threshold value P_c the critical parameter values for the onset of pulsations and for the minimal stand-off distance merge and the left branch becomes completely unstable. For $P > P_c$ the neutral stability boundary moves to the right branch and stable solutions exist only for parameter values located on the right branch of the dependence of $h(\dot{m})$ for $\dot{m}$ exceeding the critical value for the loss of stability shown with square (as it can be seen in Fig. 2 for $P = 10$ bar).

In Figure 3, the amplitudes of oscillations of local peaks of temperature, molar fractions of H and OH radicals are plotted versus time for $\phi = 2$, $\dot{m} = 2$ kg/m^{2}s, and $P = 5$ bar with solid, dotted and dashed lines,

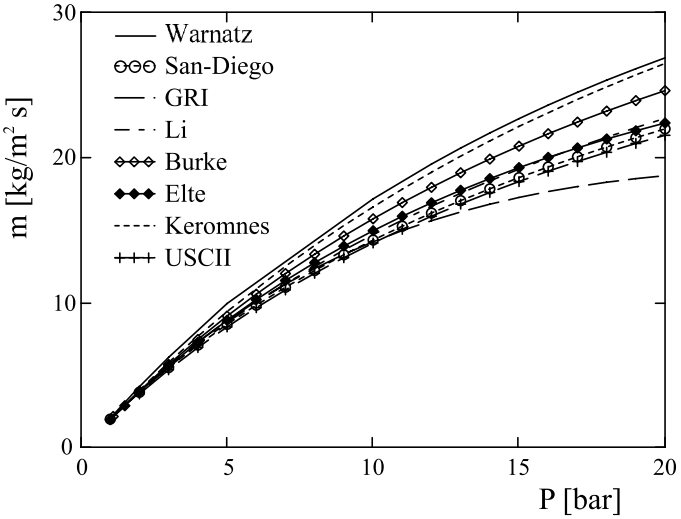

FIGURE 5. The dependence of the mass flow rate, $\dot{m}$, on the pressure, P, for $\phi = 2$ and different reaction mechanisms.

respectively. The distance of the local peaks of temperature and the molar fraction X_{H} from the burner surface for the pulsating solution is shown in Figure 4 for the same choice of parameters with the dashed and the solid lines, respectively. It should be noted that the perturbation of the temperature field in the pulsating flame can reach the order of 100 K in magnitude and hundreds of microns in longitude as is seen from the Figures 3 and 4. The time histories of peak values of X_{H} and X_{OH} demonstrate even larger relative variations over an order in magnitude.

3.2. Dependence on the kinetic schemes

In this section, we focus on the analysis of the sensitivity of the critical phenomena, blow-off and the onset of pulsations, on the specific kinetic mechanism employed in numerical scheme. The blow-off occurs as $\dot{m}$ is increased up to the value of the mass flow rate for deflagration wave as it is demonstrated in the Section 3.1. In Figure 5, we plot the dependence of $\dot{m}$ for freely propagating combustion wave on the ambient pressure for normal initial temperature of fresh mixture. We use these values as estimates of the critical conditions for the blow-off of the burner stabilized flames. As it seen in figure the general tendency is the divergence of predictions of different reaction mechanisms for increasing pressure, although more recently developed kinetic models tend to better agree with each other *e.g.* mechanisms of Li [24], San-Diego [31], and Elte [35], USCII [36] give very close predictions.

In order to investigate the onset of the oscillations the steady solutions for given ambient pressure and reaction mechanism are numerically found. The mass flow rate is gradually decreased until small oscillations of temperature and species concentrations profiles emerge. The corresponding values of the blow-off value $\dot{m}_b$, the onset value $\dot{m}_p$ for pulsations and frequency f are thus determined for every kinetic model considered in this work.

It is known [27] that the frequency scales with the characteristic time scale for the deflagration wave, $\tau \sim \kappa/u_f^2$, where κ is the thermal diffusivity and u_f is a linear flame speed with respect to the fresh mixture. The flame speed can be expressed as $\dot{m}/\rho_0$, where $\dot{m}$ is mass flow rate for deflagration wave and ρ_0 is the density of the fresh mixture. Thus the frequency of pulsations, f, is strongly interdependent with the mass flow rate for deflagration wave. In order to eliminate this relation we scale f over $\dot{m}^2$ *i.e.* we introduce $\nu = f\dot{m}^{-2}$.

The predictions of characteristics for the onset of pulsations obtained with different reaction mechanisms are summarized in Figure 6. For every reaction mechanism we collect the data of critical parameters for blow-off,

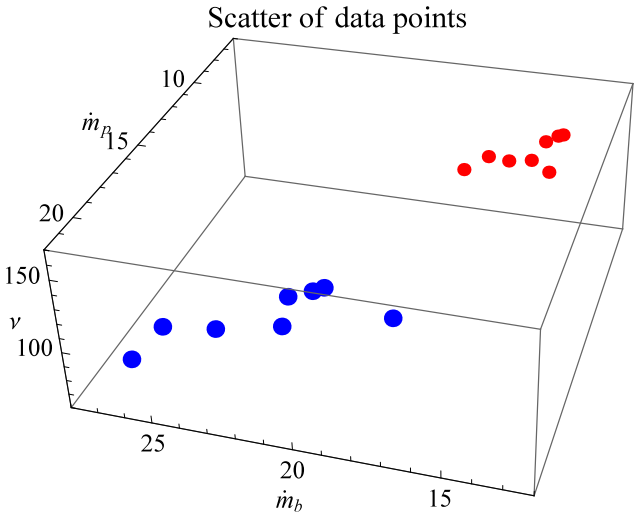

FIGURE 6. Schematic diagram of scatter of the data set for the parameter vector **M** for different values of pressure $P = 10$ bar (*small red circles*) and $P = 20$ bar (*large blues circles*).

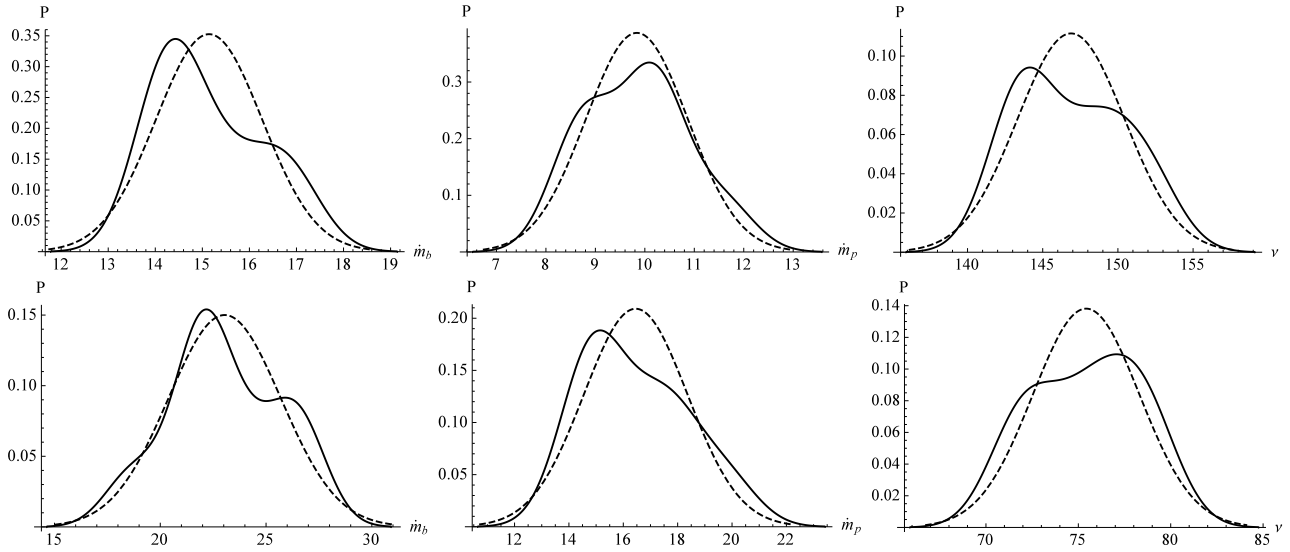

FIGURE 7. The smoothed histogram of the parameter distributions (*solid lines*) and relevant normal distributions with corresponding estimated means and variances for different pressures (upper 10 bar and lower 20 bar).

$\dot{m}_b$, onset of pulsations, $\dot{m}_p$, and scaled frequency, ν, into the vector with coordinates $\mathbf{M} = \{\dot{m}_b, \dot{m}_p, \nu\}$. Thus, we obtain the data set **M** for different mechanisms and pressures. This data set is presented in Figure 6 in three dimensional plot for two values of pressure $P = 10$ bar (red circles) and $P = 20$ bar (large blues circles). Every circle in this figure corresponds to certain reaction mechanism. It is clearly seen that the data corresponding to various reaction mechanisms is scattered in rather random manner along all three coordinates for both $P = 10$ and 20 bar. At the same time, if we consider the results for different mechanisms for a single set of parameters, calculate mean and variance, and compare the distribution of the parameter with the normal distribution, then it is seen that the data distribution is close to a normal one (see Fig. 7). However, the smoothed diagrams of the

data distribution show two local centers of accumulation for all parameters investigated. This means there is an internal similarity of the recently developed mechanisms which partly inherit kinetic data of earlier developed mechanisms.

Note additionally, on purpose we do not specify what point corresponds to which mechanism just because there is no yet reference experimental values to validate them and make a reliable verification. As it is discussed above, $\dot{m}_b$ is directly related to the laminar burning velocity of the hydrogen-air mixture and can be considered as a standard parameter for mechanism validation. However, the other two parameters, $\dot{m}_p$, and ν, are new and can be employed as an additional tests for the verification of the reaction mechanisms.

4. Conclusions

In this work, the planar hydrogen-air flames stabilized over the flat porous burner are analyzed numerically within the model with detailed reaction mechanism. The main focus is made on the study of the dynamics of flame oscillations. It is found that two types of critical phenomena may occur in the system. The steady planar solution exhibits either blow-off if the mass flow rate of the gas mixture through the porous burner approaches the value corresponding to the freely propagating deflagration wave. Alternatively the steady solution may exhibit the loss of stability due to the pulsating instabilities if the mass flow rate of the fresh gas mixture supplied through the burner is decreased up to a certain critical value. It is found that for normal and moderately elevated pressure there exist two stable steady solutions for the same values of the flame height within certain range of h variation. However, as the pressure is sufficiently increased, only the solution branch which exhibits blow-off remains stable.

The dynamics of flame oscillations is studied in detail. The onset of pulsations is supercritical. The amplitude of oscillations grows in a continuous way as the mass flow rate decreases below the critical value for the onset of oscillations. Further decrease of the mass flow rate of the fresh mixture results in the change of the character of pulsations to more relaxational. It is found also that the temperature field is significantly distorted by the onset of pulsations. There appears a local peak of temperature which can oscillate with the amplitude of the order of 100 K. The temperature disturbance along the spatial coordinate orthogonal to the burner can attain several hundreds of microns in longitude. The amplitude of oscillations of the local peak of radicals can be also significant. For example for molar fraction of OH radicals it can be as high as an order in magnitude. Thus we may expect that such strong oscillations of temperature and concentration of species profiles should be experimentally detectable.

The dependence of the characteristics of flame oscillations, the frequency and critical mass flow rate, as well as the dependence of the critical mass flow rate for the blow-off, on the choice of the reaction mechanism are analyzed. It is shown that the scaled frequency and the critical parameter values are sensitive to the reaction mechanism employed in the numerical calculations. They are also found to be statistically independent *i.e.* can be used separately for mechanism validation as additional tests to the standard protocols of the kinetics verification.

Acknowledgements. The authors acknowledge the support from DFG-RFBR grant number 17-53-12018 (RFBR)/ BY 94/2 – 1 (DFG). VVG acknowledges the support of RFBR grant numbers 17-01-00070, 16-03-00758.

References

[1] J.I. Blackshear Jr., J.W. Mapp and M. Gorman, An experimental study of pulsating low pressure flames. *Combust. Sci. Technol.* **35** (1984) 311–315.

[2] J.P. Botha and D.B. Spalding, The laminarflame speed of propane/air mixtures with heat extraction from the flame. *Proc. R. Soc. Lond. A* **225** (1954) 71–96.

[3] J. Buckmaster, Stability of the porous plug burner flame. *SIAM J. Appl. Math.* **43** (1983) 1335–1349.

[4] M.P. Burke, M. Chaos, Y. Ju, F.L. Dryer and S.J. Klippenstein, Comprehensive h2/o2 kinetic model for high-pressure combustion. *Int. J. Chem. Kinetics* **44** (2012) 444–474.

[5] B.H. Chao, Instability of burner-stabilized flames with volumetric heat loss. *Combust. flame* **126** (2001) 1476–1488.

[6] E.W. Christiansen, C.K. Law and C.J. Sung, Steady and pulsating propagation and extinction of rich hydrogen/air flames at elevated pressures. *Combust. flame* **124** (2001) 35–49.

[7] E.W. Christiansen, C.J. Sung and C.K. Law, Pulsating instability in near-limit propagation of rich hydrogen/air flames. *Symp. (Int.) Combust.* **27** (1998) 555–562.
[8] J.F. Clarke and A.C. McIntosh, The influence of a flameholder on a plane flame, including its static stability. *Proc. R. Soc. Lond. A* **372** (1980) 367–392.
[9] P. Deuflhard, E. Hairer and J. Zugck, One-step and extrapolation methods for differential-algebraic systems. *Numer. Math.* **51** (1987) 501–516.
[10] P. Deuflhard and U. Nowak, Extrapolation Integrators for Quasilinear Implicit ODEs. Springer (1987).
[11] F.N. Egolfopoulos, N. Hansen, Y. Ju, K. Kohse-Hinghaus, C.K. Law and F. Qi, Advances and challenges in laminar flame experiments and implications for combustion chemistry. *Prog. Energy Combust. Sci.* **43** (2014) 36–67.
[12] M. El-Hamdi, M. Gorman, J.W. Mapp and J.I. Blackshear Jr., Stability boundaries of periodic models of propagation in burner-stabilized methane-air flames. *Combust. Sci. Technol.* **55** (1987) 33–40.
[13] V. Giovangigli, Mass conservation and singular multicomponent diffusion algorithms. *Impact Comput. Sci. Eng.* **2** (1990) 73–79.
[14] V. Giovangigli and A. Ern, Multicomponent transport algorithms, in Vol. 24 of *Lecture Notes in Physics*. (1994).
[15] M. Gorman and S. Perrollier, Unusual pulsating states in hydrocarbon-oxygen premixed flames. *Chaos* **16** (2006) 043124.
[16] G. Goyal, U. Maas and J. Warnatz, Simulation of the behavior of rich hydrogen-air flames near the flammability limit. *Combust. Sci. Technol.* **105** (1995) 183–193.
[17] V.V. Gubernov, V. Bykov and U. Maas, Hydrogen/air burner-stabilized flames at elevated pressures. *Combust. Flame* **185** (2017) 44–52.
[18] J.O. Hirschfelder, C.F. Curtiss and D.E. Campbell, The theory of flames and detonations. Vol. 4 of *The International Symposium of Combustion*. Elsevier (1953) 190–211.
[19] G. Joulin, Flame oscillations induced by conductive losses to a flat burner. *Combust. Flame* **46** (1982) 271–281.
[20] A. Kéromnès, W.K. Metcalfe, K.A. Heufer, N. Donohoe, A.K. Das, C-J. Sung, J. Herzler, C. Naumann, P. Griebel, O. Mathieu, M.C. Krejci, E.L. Petersen, W.J. Pitz and H.J. Curran, An experimental and detailed chemical kinetic modeling study of hydrogen and syngas mixture oxidation at elevated pressures. *Combust. Flame* **160** (2013) 995–1011.
[21] D.A. Knyazkov, A.M. Dmitriev, T.A. Bolshova, V.M. Shvartsberg, A.G. Shmakov and O.P. Korobeinichev, Structure of premixed h2/o2/ar flames at 1–5 atm studied by molecular beam mass spectrometry and numerical simulation. *Proc. Combust. Inst.* **36** (2017) 1233–1240.
[22] V.N. Kurdyumov and M. Matalon, The porous-plug burner: Flame stabilization, onset of oscillation, and restabilization. *Combust. Flame* **153** (2008) 105–118.
[23] V.N. Kurdyumov and M. Sánchez-Sanz, Influence of radiation losses on the stability of premixed flames on a porous-plug burner. *Proc. Combust. Inst.* **34** (2013) 989–996.
[24] J. Li, Z. Zhao, A. Kazakov and F.L. Dryer, An updated comprehensive kinetic model of hydrogen combustion. *Int. J. Chem. Kinetics* **36** (2004) 566–575.
[25] U. Maas and J. Warnatz, Ignition processes in hydrogen-oxygen mixtures. *Combust. Flame* **74** (1988) 53–69.
[26] U. Maas and J. Warnatz, Ignition processes in carbon-monoxide-hydrogen-oxygen mixtures. Vol. 22 of *The International Symposium of Combustion*. Elsevier (1989) 1695–1704.
[27] S.B. Margolis, Bifurcation phenomena in burner-stabilized premixed flames. *Combust. Sci. Technol.* **22** (1980) 143–169
[28] S.B. Margolis, Effects of selective diffusion on the stability of burner-stabilized premixed flames. Vol. 18 of *The International Symposium of Combustion*. Elsevier (1981) 679–693.
[29] B.J. Matkowsky and D.O. Olagunju, Pulsations in a burner-stabilized premixed plane flame. *SIAM J. Appl. Math.* **40** (1981) 551–562
[30] S. Prucker, W. Meier and W. Stricker, A flat flame burner as calibration source for combustion research: Temperatures and species concentrations of premixed h2/air flames. *Rev. Sci. Inst.* **65** (1994) 2908–2911.
[31] A.L. Sánchez and F.A. Williams, Recent advances in understanding of flammability characteristics of hydrogen. *Prog. Energy Combust. Sci.* **41** (2014) 1–55.
[32] G.P. Smith, D.M. Golden, M. Frenklach, N.W. Moriarty, B. Eiteneer, M. Goldenberg, C.T. Bowman, R.K. Hanson, S. Song, W.C. Gardiner Jr V.V. Lissianski and Z. Qin, Gri-mech 3.0 (1999).
[33] D.B. Spalding and P.L. Stephenson, Laminar flame propagation in hydrogen+ bromine mixtures. *Proc. R. Soc. Lond. A* **324** (1971) 315–337.
[34] G. Stahl and J. Warnatz. Numerical investigation of time-dependent properties and extinction of strained methane and propane-air flamelets. *Combust. Flame* **85** (1991) 285–299.
[35] T. Varga, T. Nagy, C. Olm, I.Gy. Zsély, R. Pálvölgyi, É. Valkó, G. Vincze, M. Cserháti, H.J. Curran and T. Turányi, Optimization of a hydrogen combustion mechanism using both direct and indirect measurements. *Proc. Combust. Inst.* **35** (2015) 589–596.
[36] H. Wang, X. You, A.V. Joshi, S.G. Davis, A. Laskin, F. Egolfopoulos and C.K. Law, USC mech version II. High-temperature combustion reaction model of H2/CO/C1-C4 compounds (2007)